Journal of Solid State Chemistry 181 (2008) 2171–2177

Contents lists available at ScienceDirect

Journal of Solid State Chemistry

journal homepage: www.elsevier.com/locate/jssc

Structure and morphology controllable synthesis of Ag/carbon hybrid with ionic liquid as soft-template and their catalytic properties

Shu Ying Wu, Yun Sheng Ding *, Xiao Min Zhang, Hai Ou Tang, Long Chen, Bo Xuan Li

School of Chemical Engineering, Hefei University of Technology, Hefei 230009, People's Republic of China

ARTICLE INFO

Article history:
Received 17 January 2008
Received in revised form
17 March 2008
Accepted 6 May 2008
Available online 14 May 2008

Keywords:
Ionic liquid
Selective synthesis
Ag/carbon hybrid
Catalysis

ABSTRACT

Ag/carbon hybrids were fabricated by the redox of glucose and silver nitrate ($AgNO_3$) in the presence of imidazolium ionic liquid ($[C_{14}mim]BF_4$) under hydrothermal condition. Monodisperse carbon hollow sub-microspheres encapsulating Ag nanoparticles and Ag/carbon cables were selectively prepared by varying the concentration of ionic liquid. Other reaction parameters, such as reaction temperature, reaction time and the mole ratio of silver nitrate to glucose, play important roles in controlling the structures of the products. The products were characterized by XRD, TEM (HRTEM), SEM, energy-dispersive X-ray spectroscopy (EDX), FTIR spectroscopy and a Raman spectrometer. The possible formation mechanism was proposed. The catalytic property of the hybrid in the oxidation of 1-butanol by H_2O_2 was also investigated.

1. Introduction

Hybrid core–shell nanoparticle or sub-microparticle represents a new kind of structure, which has attracted much attention and has been intensively investigated in recent years. They possess interesting and special properties which are due to their improved physical and chemical properties over their single-component counterparts. Core–shell spheres encapsulating various materials have drawn considerable attention because of their applications in many fields such as electrons, magnetism and optics [1]. In addition, as a new type of one-dimensional nanostructure, the core–shell nanocables have also attracted broad interest, because their functions can be further enhanced by fabricating the core and sheath components from different materials [2–7].

Various strategies have been developed to produce nanocables and core–shell spheres. Sastry and co-workers have used chloroform as a reaction medium to synthesize core–shell Ag–Au nanoparticles by the replacement reactions between hydrophobic spherical Ag nanoparticles and hydrophobized $AuCl_4$ in toluene [8]. Colloidal carbon spheres and their core/shell structures with noble-metal nanoparticles have been fabricated by Sun and Li [1]. Meanwhile, the nanocables have also been developed quickly. They have been synthesized by high-energy input approaches, including the chemical vapor deposition route and the carbothermal reduction method [9,10]. In addition, several mild chemistry methods emerge, for example, a series of work of synthesis of carbon-based nanocables by the one-pot hydrothermal technique have been realized [11–17]; polypyrrole/poly(methyl methacrylate) coaxial nanocables have been synthesized by the sequential polymerization of monomers within the channels of mesoporous silica, followed by dissolution of the template [18].

The noble metals in nanoscales have become a subject of intense interest in various fields because of their outstanding properties. It has been experimentally demonstrated that metal nanoparticles have high catalytic activities for hydrogenation, oxidation, carbonylation, etc. [19–24]. For example, silver nanoparticles catalyze the reduction of aromatic nitro compounds [25]. However, they would often congregate during catalytic processes. The reason is that nano-sized metal particles are active and prone to coalesce due to van der Waals forces and high surface energy unless they are protected. The structure of supporting materials plays an important role in the activity of the catalyst. Carbon spheres and carbon nanotubes, because of their interesting properties and large surface area, have been receiving increasing attention for their application in catalyst support [26].

Herein, we report a controllable method to prepare Ag/C nanocables and carbon hollow spheres encapsulating Ag nanoparticles in their cores. In the experiment, one kind of imidazolium ionic liquid, 1-*n*-tetradecyl-3-methylimidazolium tetrafluoroborate ($[C_{14}mim]BF_4$), was used as the soft-template to prepare the hybrid. We can alternatively obtain Ag/C nanocables or carbon hollow spheres encapsulating Ag nanoparticles in their cores by altering the concentration of $[C_{14}mim]BF_4$, which realized the controllable synthesis of Ag/C hybrids. Meanwhile, the catalysis in the oxidation of 1-butanol by H_2O_2 was also investigated.

* Corresponding author. Fax: +86 551 2901545.
E-mail address: dingys@hfut.edu.cn (Y.S. Ding).

0022-4596/$ - see front matter © 2008 Elsevier Inc. All rights reserved.
doi:10.1016/j.jssc.2008.05.006

2. Experimental section

2.1. Preparation of $[C_{14}mim]BF_4$

All chemical reagents were of analytic purity and they were used without further purification. The imidazolium ionic liquid, 1-*n*-tetradecyl-3-methylimidazolium tetrafluoroborate ($[C_{14}mim]BF_4$), was synthesized by the ionic exchange reaction between 1-*n*-tetradecyl-3-methylimidazolium bromide ($[C_{14}mim]Br$) and NH_4BF_4. The $[C_{14}mim]Br$ was synthesized according to the literature [27].

2.2. IL-assisted hydrothermal synthesis of Ag/C nano-hybrid

Here we adopted the hydrothermal carbonization co-reduction process (HCCR) [28] to synthesize Ag/C hybrids. In the process, 0.5 g $[C_{14}mim]BF_4$ and 0.5 g glucose were dissolved in 35 ml distilled water. Then, 0.5 ml of 0.1 M $AgNO_3$ was added in dropwise manner under vigorous magnetic stirring. The solution turned yellow. Followed by 5 min of agitation, the solution was transferred into a 50 ml Teflon-lined stainless steel autoclave, which was sealed and maintained at 180 °C for 3 h and then air-cooled to room temperature. The resulting suspension was centrifugated at 3000 rpm for 30 min to obtain a black precipitate, which was then washed by distilled water. The product was re-dispersed in absolute ethanol for characterization.

2.3. The catalysis in the oxidation of 1-butanol by H_2O_2

The 0.01 g products prepared by the process described above were added into a 100 ml three-neck round flask, and then 20 ml 1-butanol was introduced into the flask. The mixture was treated ultrasonically for about 15 min, which could make the particles disperse better in the 1-butanol. The 20 ml H_2O_2 was dripped with the dropping funnel when the system was heated to 80 °C. The mixture was stirred for 8 h at 80 °C. After 8 h of reaction, the mixture was cooled naturally. Then the catalyst was removed by centrifugation. There are two delaminations and the super stratum was spilled for characterization.

2.4. Characterization

The particle size and morphology of the resulting products were characterized using a field emission SEM (X-650 made by HITACHI), operating at accelerating voltages of 20 kV and transmission electron microscopy (TEM) (H-800) at accelerating voltages of 100 kV. High-resolution TEM images were obtained on a JEOL-2010 high-resolution electron microscope at accelerating voltages of 200 kV. This instrument was equipped with an energy-disperse X-ray spectroscopy (EDX) system. The powder X-ray diffraction (XRD) patterns were recorded on a D/Max-rB diffractometer (Rigaku, Japan) with Cu$K\alpha$ ($\lambda = 1.5406$ Å). The samples were also characterized by FTIR spectroscopy (NICOLET MAGNA-750) and a Raman spectrometer (RAMANLOG6). The oxidative products were characterized by FTIR spectroscopy (NICOLET MAGNA-750). The gas chromatograph, which was used to measure the conversion of the 1-butanol, was GC-9A (SHIMADZU, Japan).

3. Results and discussion

3.1. Characterization of the silver nanoparticles

Fig. 1a shows the scanning electron microscopy (SEM) image, which shows that the products consist of spheres. Fig. 1b shows a typical TEM image of the Ag/C hybrid, indicating that the products consist of hollow spheres with Ag nanoparticles encapsulating in their cava. The diameter of the hollow spheres is about 346 nm and the shell thickness is 114 nm. The diameter of Ag nanoparticles here is about 25 nm. We could also find that the hollow spheres are uniform in size. We have taken the photographs of a single sphere from different directions. The sphere in Fig. 1c is the same as in Fig. 1d. The two pictures show that the center of the sphere is hollow and the silver nanoparticle encapsulating in the cava lies on the wall of the shell.

Fig. 2 shows a typical XRD pattern of the products and the primary peaks marked with rhomboids can be indexed to the diffraction of (111), (200) and (220) planes of fcc silver. We can observe that there are also peaks of AgBr, which are marked with asterisks in the pattern. The diffraction peak of the (200) plane of silver metal appeared at 44.30°. And its position is so close to the (220) peak of AgBr (2θ, 44.61°) that they could not be differentiated under the experimental conditions. The ionic liquid we used was synthesized by ionic exchange between $[C_{14}mim]Br$ and NH_4BF_4. The residual bromine ions can react with $AgNO_3$, therefore forming AgBr. Silver bromide might play an important role in the formation of Ag nanoparticles, which will be illustrated in the following text. The wide and weak peak around 20° can be indexed to amorphous carbon.

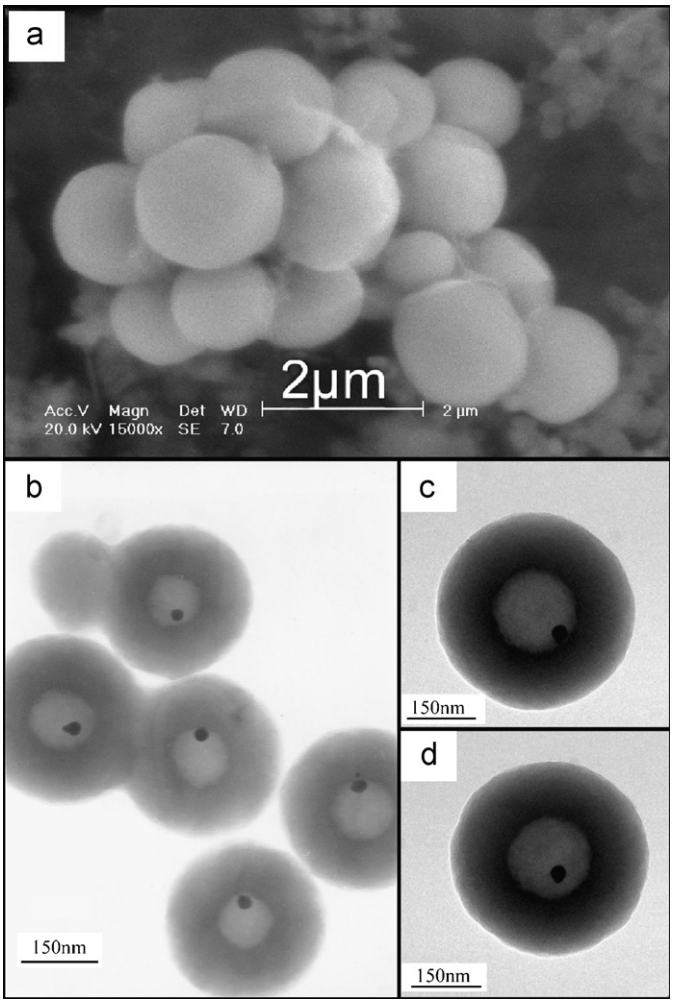

Fig. 1. SEM and TEM images of the Ag/carbon products prepared at 180 °C for 3 h: (a) the representative SEM picture; (b) TEM picture of the hollow spheres with Ag nanoparticles in their cores; (c) and (d) are the TEM pictures of a single sphere.

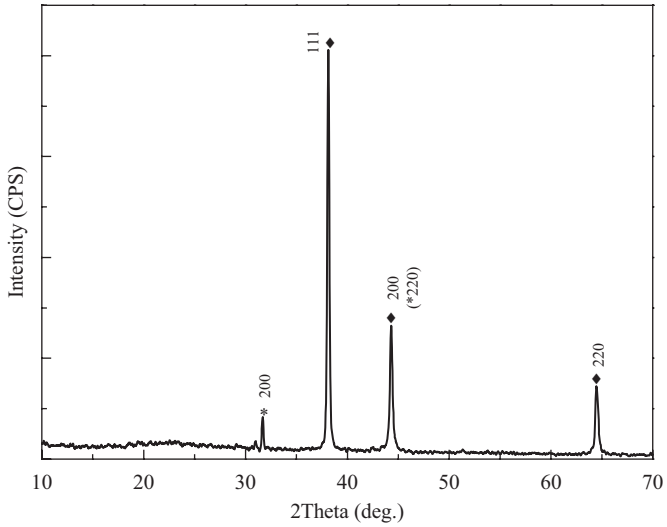

Fig. 2. XRD pattern of the as-prepared Ag/carbon products.

To our surprise, we detected a novel structure after detailed TEM observation. There are some spheres that are linked by thin wires. Fig. 3a is the picture taken at a relatively low magnification. From it we can find that there are thin wires, which assemble the hollow spheres into a novel and interesting structure. In order to know the structure, we detected it by high-resolution TEM. Fig. 3b is the image. It can be easily observed that the thin wire is just the extension of the shell. The contrast between the inner and the outer of the wire can be observed and it is due to the different thicknesses.

We used energy-dispersive X-ray analysis (EDX) to investigate the elemental composition of the noble-metal-loaded hollow spheres. Fig. 3d1 is the energy-dispersive X-ray spectra taken from the nanoparticles in the inner side of the spheres. It illustrates that the nanoparticles are made of metallic silver and carbon. In our reaction system, the concentration of $AgNO_3$, which was the silver source, was low and the quantity of glucose was relatively excessive compared to $AgNO_3$. Therefore, we can find from the spectra that the content of carbon was much higher. Fig. 3d2 shows the elemental composition of the shell of the hollow spheres. It is constituted only by element carbon, and the existed element oxygen derives from glucose.

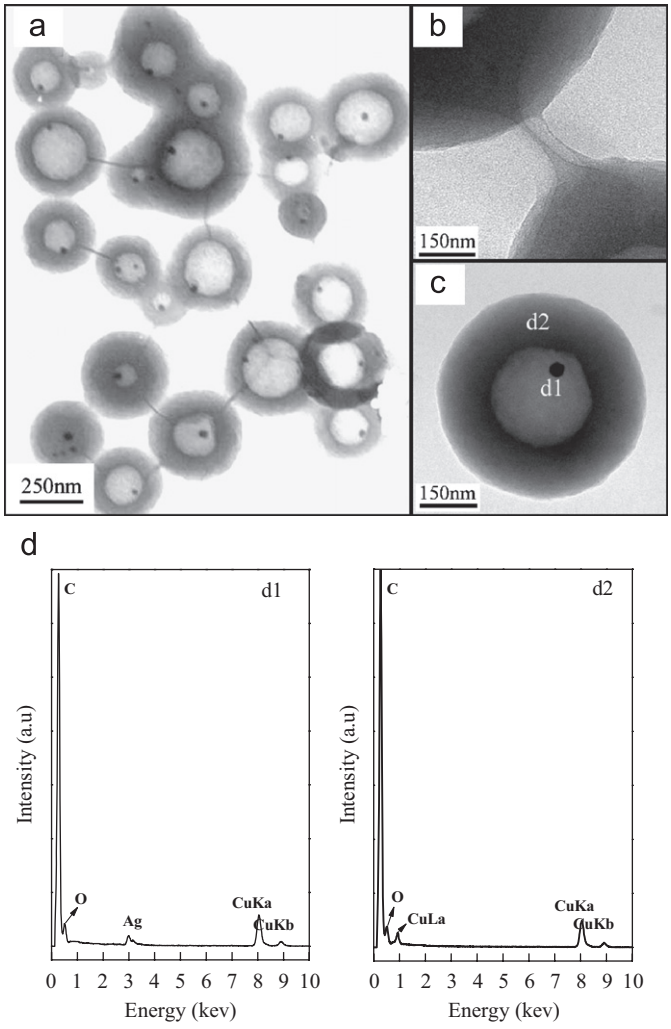

Fig. 3. TEM images of the Ag/carbon products: (a) panoramic view of the assembled structure at relative low magnification, (b) high-resolution TEM picture of an assembled wire, (c) an individual Ag/carbon hollow sphere, (d1) energy-dispersive X-ray spectrum taken from d1 area in (c) and (d2) energy-dispersive X-ray spectrum taken from d2 area in (c).

3.2. The controlled synthesis of Ag/carbon nano-hybrids

3.2.1. Effect of temperature on the structure and morphology of Ag/carbon hybrid

The typical reaction was carried out at 180 °C for 3 h and we obtained the hollow sub-microspheres loading Ag nanoparticles in their cores described as above. We varied the reaction temperature at 140, 160, 200 and 220 °C. All reactions were carried out for 3 h. We found that there were no expected products when the temperature was lower than 160 °C. The structures were irregular when the reaction was carried out at temperatures higher than 180 °C. Fig. 4a is the TEM image of the product synthesized at 200 °C. It shows that the silver nanoparticles in the cores are irregular and the sizes of the hollow spheres are uneven.

3.2.2. Effect of reaction time on the structure and morphology of the Ag/carbon hybrid

We also investigated the influence of the synthesis time on the shape of the product. Based on the observation, we found that the size of the cavity became smaller with time, that is, the shell of the hollow spheres became thicker. After the reaction time was extended to 48 h, there were many solid carbon spheres (Fig. 4b). This indicates that carbonization of glucose takes place in the inner side of the hollow spheres. There may be pores in the carbonaceous shell; therefore, glucose molecules can continuously diffuse into the inner side of the hollow spheres via capillary action [29]. As a result, with time, the hollow spheres gradually become solid spheres by the continuous carbonizing of glucose.

3.2.3. Effect of the mole ratio of $AgNO_3$ to glucose on the structure and morphology of the Ag/carbon hybrid

The proportion of $AgNO_3$ to glucose plays an important role in determining the morphology of the product. In a typical experiment, 0.5 g glucose and 0.5 ml 0.1 M $AgNO_3$ were added into the reaction system and we obtained carbon hollow submicrospheres in which the silver nanoparticles were encapsulated, and the silver nanoparticles were regular. However, the Ag particles assembled into triangle, near-cubic or other irregular silver particles when the mole ratio of $AgNO_3$ to glucose increased. For example, when the concentration of $AgNO_3$ was increased to 0.8 M, there were different irregular silver particles in

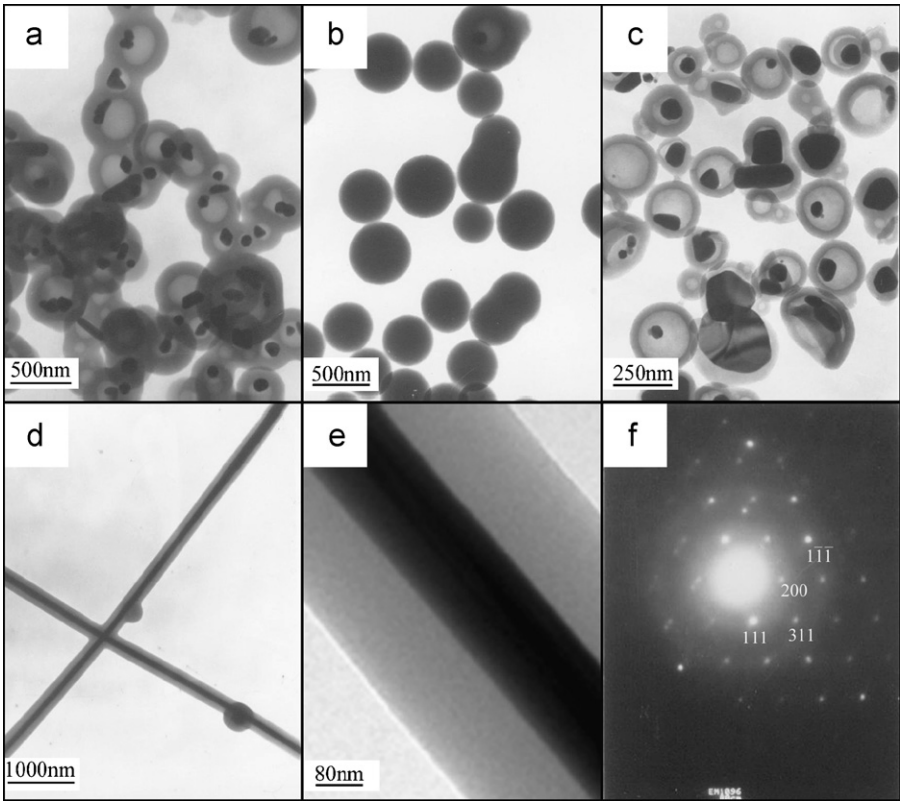

Fig. 4. Representative TEM images of the Ag/carbon products prepared at (a) 200 °C, 3 h; (b) 180 °C, 48 h; (c) the $AgNO_3$ concentration was increased to 0.8 M and (d) the dosage of $[C_{14}mim]BF_4$ was reduced to 0.1 g while the other reaction parameters were the same as the typical experiment; and (f) electron diffraction pattern taken from an individual cable (e).

the carbon hollow sub-microspheres as shown in Fig. 4c. Fig. 4c also shows that the thickness of the shell became thinner (about 47 nm) when the mole ratio of $AgNO_3$ to glucose increased.

3.2.4. *Effect of the ionic liquid's concentration on the structure and morphology of the Ag/carbon hybrid*

Among the various parameters, the concentration of the soft-template is particularly crucial for the control of the structure and morphology of the particles. We gained hollow spheres when 0.5 g ionic liquids were added in the typical reaction. In order to explore the function of ionic liquid in determining the structure and morphology of the hybrids, we reduced the dosage of $[C_{14}mim]BF_4$ to 0.1 g. It was interesting that we obtained Ag/C cables with diameters of 360 nm. The silver cores are straight and uniform in diameter (around 112 nm) throughout their entire length (shown in Fig. 4d). Fig. 4e is an individual cable and its electron diffraction pattern is shown in Fig. 4f with the electron beam focused perpendicularly on the surface $(0\bar{2}2)$. The SAED pattern indicates the single-crystalline nature of the Ag core.

3.3. *Formation mechanism of the Ag/carbon hybrids*

3.3.1. *The reaction in our system*

The temperature 180 °C is higher than the normal glycosidation temperature and it leads to aromatization and carbonization [1]. Under the hydrothermal condition, various chemical reactions of glucose can take place and result in a complex mixture of organic compounds [17]. After hydrothermal treatment, the resulting solution took an orange color. This phenomenon was consistent with the work of Sun and Li [1]. Thereby, we believed the carbonization of glucose took place and produced some aromatic compounds and oligosaccharides in our experiment. The FTIR spectrum of the hybrid (Fig. 5a) shows that there are residual hydroxyls after the hydrothermal treatment. And according to the spectrum, we find that C═O and C═C groups exist in the product, which supports the concept of aromatization of glucose during the hydrothermal reaction. From the FTIR spectrum, we can also see the weak vibration at 1377 and 1463 cm^{-1}. They can be attributed to COO^- groups, which indicate the occurrence of redox reactions. The group of CHO of glucose acts as a reductive group while silver ion plays the role of an oxidant.

We used Raman spectra analysis to observe the structure of the carbon shell of the hollow spheres. There was a strong peak at 1580 cm^{-1} (Fig. 5b), which was attributed to the in-plane vibrations of crystalline graphite. From the spectra we can also detect that there was a weak peak at 1360 cm^{-1}, which was attributed to disordered amorphous carbon.

In our approach, glucose acts as the carbon source and reducing agent, while the noble-metal salt, $AgNO_3$, acts as the source of the metal to be encapsulated. The silver nitrate has been confirmed to be the catalyst of the saccharide's carbonization under suitable hydrothermal condition [28]. The carbonization of glucose and the redox between $AgNO_3$ and glucose took place indeed according to the above discussion.

3.3.2. *Mechanism for the formation of the Ag/carbon hybrid*

A possible formation mechanism is schematically illustrated in Fig. 6. The silver ions interact with the glucose molecules and are deoxidized by glucose to small Ag nanocrystals. The residual bromine ions react with the silver ions and result in the AgBr crystal, which offers the nucleation center, and then the small Ag

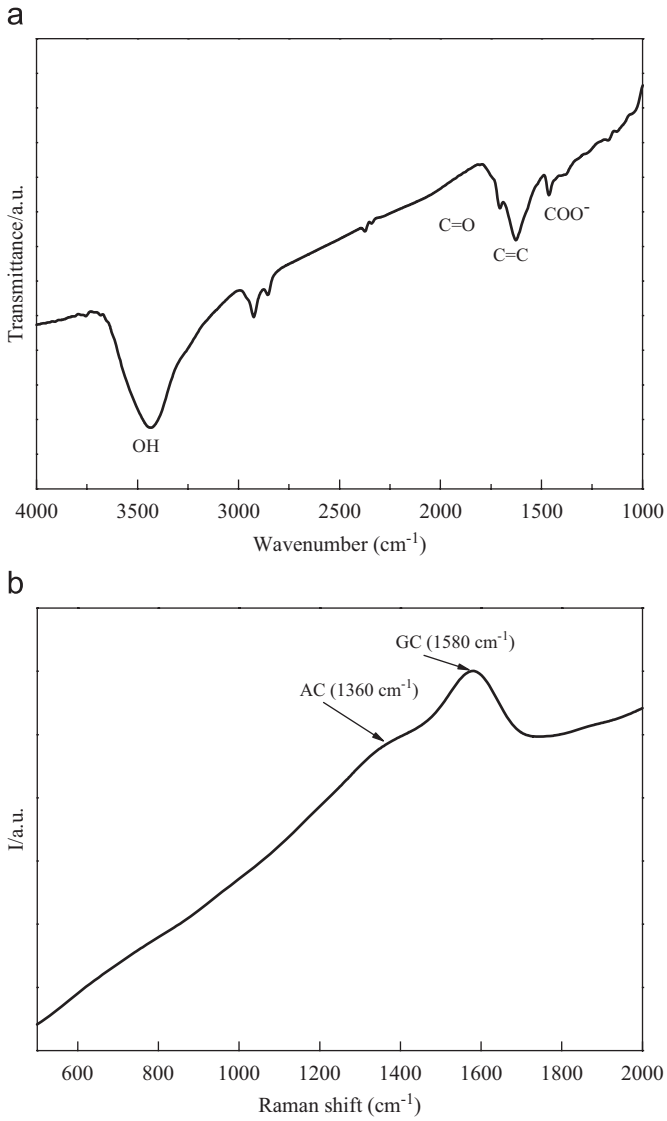

Fig. 5. (a) FTIR spectra of the Ag/carbon hybrid particles and (b) Raman spectra of the Ag/carbon hybrid particles.

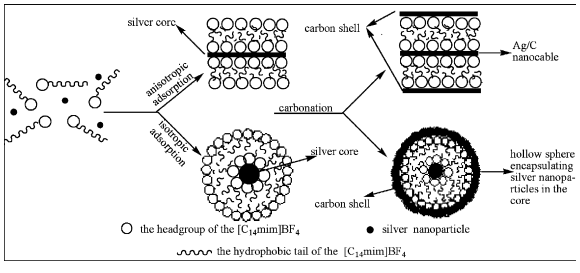

Fig. 6. The schematic formation of the Ag/carbon structure.

nanocrystals aggregate onto AgBr to form Ag nanoparticles. Once the Ag nanoparticles appear, they are captured by the organic cations of the ionic liquid. According to the work of Chen's group [30], we suppose that the adsorption and structural configuration of the ionic liquid on the surface of the Ag nanoparticles are similar to CTAB (cetyltrimethylammonium bromide) on the surface of the Ag nanoparticles. The headgroups of the organic cations of the ionic liquid adsorb on the surface of the nanoparticles, the hydrophobic tails are tilted to the surface to form micelles in the water solution. And there is an ionic liquid bilayer on the silver nanoparticles. The bilayer adsorbed on Ag clusters makes Ag nanoparticles positively charged and the resulted electrostatic repulsion prevents micelles from aggregating. Under the hydrothermal condition, glucose can be carbonized and the micelles serve as the charing core. The carbon spheres that cap the micelle then form Ag particles that remained in the core of the spheres.

The reaction in the absence of ionic liquid only brought about irregular solid spheres. Hence we believe that ionic liquid acts as a soft-template, which has the effects of a shape controller and a stabilizing agent in the reaction. During the reaction, ionic liquid adsorbs on the silver crystal faces and the adsorption characteristics depend on its concentration. The result shows that when the concentration of the surfactant is reduced to one-fifth of that of the typical reaction, the surfactant would adsorb anisotropically on the silver crystal faces, which direct the silver metal to grow into linear structures. While the ionic liquid adsorbs uniformly on the silver crystal faces in the typical synthesis, the crystal grows into spherical particles. In the typical experiment, the wires that linked the spheres were supposed to be formed by carbonation directed by rod micelles. The majority of $[C_{14}mim]BF_4$ adsorbed on the surface of the silver crystal and formed a bilayer. Meanwhile, there were also some surfactants that arranged in rod micelles. The rod micelles offered the carbonation center to form carbon wires.

3.4. Catalysis of Ag/carbon hybrid in the oxidation of 1-butanol

Since the Ag/C hybrid with a core–shell structure could act as highly dispersed electrodes, they should help in the electron transfer between the alcohols and oxidant donors, so they could have the catalytic effects on the oxidation of alcohols. Here we selected 1-butanol and H_2O_2, one kind of green oxygen donors, to study the catalysis of Ag/C nano-hybrids with the hollow sphere structure in the reaction of alcohol oxidation.

Fig. 7 shows the FIIR spectrum of the oxidation product. We can see that the products are identical irrespective of the silver catalyst being added or not, and it shows oxidation indeed happens. When the reaction temperature was 80 °C, and 0.01 g (0.061 percent of the weight of 1-butanol) Ag/C hybrid was added, the conversion of 1-butanol in the reaction system was close to the reaction without a nano-hybrid (Table 1, entries 1 and 2). However, the silver catalysts showed effective catalytic activity in the experiment conducted at 110 °C. The conversion increased from 48.70% to 68.94% when 0.01 g catalysts were used (Table 1, entries 3 and 4). Increasing the dosage of catalysts to 0.02 g only brought about an increment of 1.1% (Table 1, entries 4 and 5), so the Ag/C hybrid has high catalytic efficiency in the oxidated reaction of 1-butanol by H_2O_2. The support, carbon shell, could prevent the silver nanoparticles from congregating. Nevertheless, it could also reduce the interface of the silver particles and the reactant, thereby leading to catalyst deactivation. In order to demonstrate this, we ultrasonically treated the reaction mixture so as to make the catalyst more dispersive. In the initial experiment, the ultrasonic treating time was 15 min. And we found that the conversion increased from 68.94% to 75.78% (Table 1, entries 4 and 6) when the treating time was extended to 1 h. So the conclusion can be drawn that the pretreatment that excited the catalytic activity plays an important role. Other pretreatment methods that may be more effective to explode the catalysts' activity are being studied. The catalytic process can be explained by an electrochemical mechanism, silver in the supported carbon spheres serves as an electron relay for an

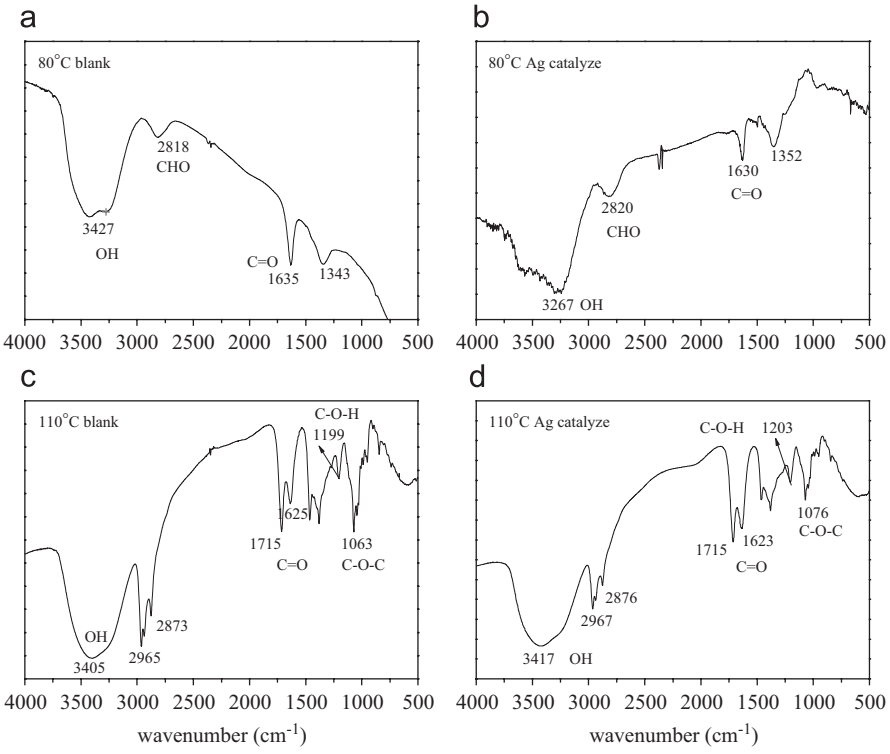

Fig. 7. FTIR spectrum of the oxidation products.

Table 1
Conversion of the oxidation of 1-butanol

Entry	Catalyst dosage (g)	Ultrasonic treating time (min)	Reaction temperature (°C)	Conversion (%)
1	0.00	15	80	37.50
2	0.01	15	80	36.70
3	0.00	15	110	48.70
4	0.01	15	110	68.94
5	0.02	15	110	70.04
6	0.01	60	110	75.78

oxidant and a reductant. The function of metal nanoparticles as a nanoelectrode makes it possible to catalyze other redox reactions via an electron transfer-storage process.

4. Conclusion

In summary, with the help of 1-*n*-tetradecyl-3-methylimidazolium tetrafluoroborate ($[C_{14}mim]BF_4$) as the soft-template, we selectively synthesized hollow carbon spheres encapsulating silver nanoparticles in their cores and Ag/C cables. These Ag/C hybrids have been obtained by the hydrothermal treatment of silver nitrate and glucose in the presence of ionic liquid. The structure could be controlled by the variation of experiment conditions such as temperature, time, mole ratio of $AgNO_3$ to glucose and the concentration of ionic liquid. We here have successfully prepared the Ag/C hybrid with core–shell structure, which shows effective catalytic activity in the oxidation of 1-butanol by the "green" oxidant H_2O_2. Furthermore, the assembly spheres will create new possibilities for preparation of novel functional materials. Thus, as the next step, the investigation and discovery of its properties such as optical, electrical, and mechanical behavior will be carried out.

Acknowledgments

We thank Prof. Jun Zhang and Zhi-gang Wang at Institute of Chemistry, Chinese Academy of Sciences (CAS) for insightful discussions on the synthesis of Ionic Liquid and its application, and also thank Dr. Qing Yang and Dr. Helin Niu at Nanochemistry and nanomaterials, Hefei National Laboratory for Physical Sciences at Microscale for their kind help on the characterization. This research is financially supported by Nature Science Foundation of Anhui Province (5044095), National Science Foundation of China (10590355), Annual Important Scientific Research Items of Anhui Province (06022016) and Important Key R&D Projects of Anhui Province (07010202025).

References

[1] X.M. Sun, Y.D. Li, Angew. Chem. Int. Ed. 43 (2004) 597.
[2] L.B. Luo, S.H. Yu, H.S. Qian, J.Y. Gong, Chem. Eur. J. 12 (2006) 3320.
[3] J.Q. Hu, Y. Bando, J.H. Zhan, D. Golberg, Angew. Chem. Int. Ed. 43 (2004) 4606; J.Q. Hu, Y. Bando, J.H. Zhan, D. Golberg, Appl. Phys. Lett. 85 (2004) 3593; J.H. Zhan, Y. Bando, J.Q. Hu, Chem. Mater. 16 (2004) 5158.
[4] Q. Li, C.R. Wang, J. Am. Chem. Soc. 125 (2003) 9892.
[5] X. Fan, X.M. Meng, X.H. Zhang, Appl. Phys. Lett. 86 (2005) 1731.
[6] S. Bae, H. Seo, H. Choi, D. Han, J. Park, J. Phys. Chem. B 109 (2005) 8496.
[7] J. Ku, R. Vidu, R. Talroze, P. Stroeve, J. Am. Chem. Soc. 126 (2004) 15022.
[8] J. Yang, J.Y. Lee, H.P. Too, J. Phys. Chem. B 109 (2005) 19208.
[9] Y.B. Li, Y. Bando, D. Golberg, Adv. Mater. 16 (2004) 93.
[10] G.W. Meng, L.D. Zhang, C.M. Mo, S.Y. Zhang, Y. Qin, S.P. Feng, H.J. Li, J. Mater. Res. 13 (1998) 2533.
[11] H.S. Qian, L.B. Luo, J.Y. Gong, S.H. Yu, T.W. Li, L.F. Fei, Crystal Growth Des. 6 (2006) 607.
[12] D.K. Ma, M. Zhang, G.C. Xi, J.H. Zhang, Y.T. Qian, Inorg. Chem. 45 (2006) 4845.
[13] J.Y. Gong, S.H. Yu, H.S. Qian, L.B. Luo, T.W. Li, J. Phys. Chem. C 111 (2007) 2490.
[14] J.Y. Gong, L.B. Luo, S.H. Yu, H.S. Qian, L.F. Fei, J. Mater. Chem. 16 (2006) 101.
[15] L.B. Luo, S.H. Yu, H.S. Qian, J.Y. Gong, Chem. Commun. (2006) 793.
[16] L.B. Luo, S.H. Yu, H.S. Qian, T. Zhou, J. Am. Chem. Soc. 127 (2005) 2822.
[17] Q. Peng, Y.J. Dong, Y.D. Li, Angew. Chem. Int. Ed. 42 (2003) 3027; T. Sakaki, M. Shibata, T. Miki, H. Hirosue, N. Hayashi, Bioresource Technol. 58 (1996) 197.
[18] J. Jang, B. Lim, J. Lee, T. Hycon, Chem. Commun. (2001) 83.
[19] F. Zaera, A.J. Gellman, G.A. Somarajai, Acc. Chem. Res. 19 (1986) 24.

[20] G.C. Bonds, Acc. Chem. Res. 26 (1993) 490.
[21] T. Pal, T.K. Sau, N.R. Jana, J. Colloid Interface Sci. 202 (1998) 30;
T. Pal, T.K. Sau, N.R. Jana, Langmuir 13 (1997) 1481.
[22] J.H. Fendler, Chem. Rev. 87 (1987) 877.
[23] T. Ahmadi, Z.L. Wang, T.C. Green, A. Henglein, M.A. El-sayed, Science 272 (1996) 1924.
[24] D.M. Hercules, A. Proctor, M. Hoopla, Acc. Chem. Res. 27 (1994) 387.
[25] N. Pradhan, Colloids Surf. A 196 (2002) 247.
[26] V. Lordi, N. Yao, J. Wei, Chem. Mater. 13 (2001) 733.
[27] Y.S. Ding, M. Zha, Colloids Surf. A 298 (2007) 201.
[28] S.H. Yu, X.J. Cui, L.L. Li, K. Li, Adv. Mater. 16 (2004) 1636.
[29] G.C. Xi, C. Wang, X. Wang, Y.T. Qian, H.Q. Xiao, J. Phys. Chem. C 112 (2008) 965.
[30] Z.M. Sui, X. Cui, Physica E 33 (2006) 308.